Potential and kinetic sputtering of alkanethiol self-assembled monolayers by impact of highly charged ions

M. Flores,* B. E. O'Rourke, and Y. Yamazaki†
Atomic Physics Laboratory, RIKEN, 2-1 Hirosawa, Wako, Saitama 351-0198, Japan

V. A. Esaulov
Laboratoire des Collisions Atomiques et Moleculaires (UMR 8625, CNRS-Universite), Universite Paris-Sud, bat 351, 91405 Orsay, France

(Received 1 October 2008; published 4 February 2009)

Highly charged ions have been used to study the sputtering of positive molecular fragments from mercaptoundecanoic acid and dodecanethiol self-assembled monolayers on gold surfaces. The samples were bombarded with Ar^{q+} $(4 \leqslant q \leqslant 10)$ ions with kinetic energies from 2 to 18 keV. The main fragments detected were H^+, $C_nH_{2n}^+$, and $C_{n+1}O_2H_{2n+1}^+$ from mercaptoundecanoic and H^+, $C_nH_{2n}^+$, and $C_{n+1}H_{2n+3}^+$ from dodecanethiol. The proton yields were increased with larger charge state q of the highly charged ion (HCI) in both samples, scaling as q^γ, with $\gamma \sim 5$. The charge state dependence is discussed in terms of electron transfer to the HCI. The final yield of protons depends on molecular functional group characteristics, orientation on the surface, and reneutralization phenomena.

DOI: 10.1103/PhysRevA.79.022902 PACS number(s): 79.20.−m, 61.66.Hq, 68.49.Sf

I. INTRODUCTION

Self-assembled monolayers (SAMs) are ordered molecular assemblies formed by the adsorption of an active surfactant on a solid surface. SAMs are a novel class of materials with promising applications in different technological fields such as nanofabrication and chemical and biological sensing [1–3]. Some frequently used compounds in SAMs are the n-alkanethiol $HS(CH_2)_nX$, where X refers to the terminal or functional end group. Specifically, SAMs with COOH functional end groups [such as mercaptoundecanoic acid (MUDA)] are used to bind metal clusters and immobilize carbon nanotubes to surfaces [2]. Alternatively, SAMs with CH_3 functional end group [such as dodecanethiol (DDT)] have been used to tune the work function of metallic surfaces [3]. The assembly characteristics of SAMs such as density functional theory and MUDA have been studied in numerous papers (see the above references) and there exist density functional theory calculations of their electronic structure [4].

Several techniques have been used to study and characterize SAMs [5], for example, scanning probe microscopies and optical and ion spectroscopies [6–10]. In the latter case, the interaction of ions with SAM surfaces leads to the sputtering of molecules from the surface, with the detection of such molecules giving information on both the chemical and structural composition of the SAM [10]. For this reason much experimental and theoretical effort has been directed towards ion-SAM collisions in order to understand the mechanism of molecular emission from these surfaces [9,11]. Furthermore, investigations of ion-SAM interactions are also interesting as model studies of well ordered organic systems with well-defined functional end groups, as a complement to studies of ion-induced damage in biomolecular systems. This field has attracted considerable attention in the last years [12] in relation to ion beam applications in cancer treatment. By changing the functional end group, SAMs allow one to address the case of progressively more complex molecular systems as building blocks of large molecules.

Recently, the interactions of highly charged ions (HCIs) with solid surfaces have been the subject of active research, including the study of the various emission processes [13] and future technological applications [14]. For slow HCIs, the potential energy stored in the projectile can far exceed its kinetic energy. In contrast to the kinetic sputtering process, which is due to momentum transfer from the ion to the surface, HCI may also transfer significant potential energy, removing ions and molecules from the surface in a process called potential sputtering [15].

There have been previous reports of SAM surfaces irradiated with HCI. Schenkel *et al.* [16] studied the secondary ion production from alkyl-SAM CF_3-phenol/Si(111) using $Xe^{10+,30+,41+}$, Au^{69+}, and Th^{73+} ions. Large yields of positive ions were obtained and subsequent observations with atomic force microscopy showed craters on the SAM surfaces, with diameters of 50–63 nm, formed by individual HCI impact. Ratliff *et al.* [17] compared effective damage on dodecanethiol/Au(111) surfaces due to irradiation with beams of Ar* and Xe^{44+} ions by comparing the change in reflectivity after etching. It was estimated that 10^5Ar* atoms are required to produce the equivalent change as one Xe^{44+} ion [17].

In this work, we have employed HCIs to study the sputtering of positive molecular fragments from two different alkanethiol SAMs, mercaptoundecanoic acid (MUDA), and dodecanethiol (DDT), formed on gold surfaces. The SAMs were bombarded with a pulsed beam of Ar^{q+} $(4 \leqslant q \leqslant 10)$ ions. Positive molecular ions were identified and analyzed from time of flight (TOF) spectra.

*marcos@riken.jp
†Also at Institute of Physics, Graduate School of Arts and Science, University of Tokyo, Tokyo, Japan.

II. EXPERIMENTAL SECTION

A. Experimental setup

HCIs were produced by the RIKEN high-T_c superconducting electron beam ion source [18]. A 60°-analyzer magnet selects the charge state of the HCIs. The measurements were made with ion beams of Ar^{q+} with $4 \leqslant q \leqslant 10$ and kinetic energy from 2.5 up to 18 keV, with a typical flux of around 500 HCIs per second.

The sample and TOF apparatus were housed in an analysis chamber which has been described in detail elsewhere [19]. All measurements were performed under UHV conditions (10^{-9} Torr). The sample was mounted on a movable and rotatable manipulator. A ground mesh was positioned 10 mm in from of the sample. In order to extract positively charged secondary ions effectively the sample was positively biased. A two-dimensional (2D) position sensitive detector (PSD) was mounted on a turntable plate coaxially with the sample holder at a distance of 140 mm from the sample. This configuration enables measurements at different incident angles. Double emission events due to single HCI impact were directly tested by analyzing the output 2D-PSD signal (preamplified) with an oscilloscope and were found to account for only around 1% of the total single event count. Neglecting double emission events as a small percent of the single events a single stop time-to-amplitude converter was used.

B. Sample preparation

The SAM samples were prepared on thin gold films which were grown on high grade $V-1$ mica. The mica was preheated to 350 °C for several hours and gold film was deposited to a depth of 200 nm at a rate of 5 nm/min at this temperature. Using this method, larger and atomically flat domains of Au(111) were obtained. Directly before use, the samples were flame annealed at 650 °C to clean off any impurities and induce surface reconstruction [20]. Scanning tunneling microscope (STM) images showed that flat terraces of length greater than 100 nm were routinely obtained. The annealed gold sample, cooled under an inert gas stream, was then placed in a millimolar solution of thiol in ultrapure (99%) ethanol at room temperature for around 20 h.

In the present experiment the thiols mercaptoundecanoic acid $HS(CH_2)_{10}COOH$ and dodecanethiol $HS(CH_2)_{11}CH_3$ were used. After removing the sample from the solution it was then rinsed in ethanol and dried under a N_2 stream before finally being inserted into the analysis chamber. STM observations of the MUDA and DDT samples show well ordered molecular domains separated by domain boundaries and vacancy islands in agreement with previous reports [7]. While molecular resolution images were not easily obtainable for MUDA surfaces, DDT samples routinely showed the characteristic $(\sqrt{3}\times\sqrt{3})R30°$ and $c(4\times2)$ reconstructions [7].

C. TOF spectra

In order to correctly determine the masses corresponding to of each peak, time of flight (TOF) spectra at several sample (acceleration) voltages (V_s) were taken. Typical positive ion spectra from DDT for two different V_s are shown in Fig. 1. It is observed that the peak positions are shifted with changing sample voltage, increasing V_s decreases the time of flight.

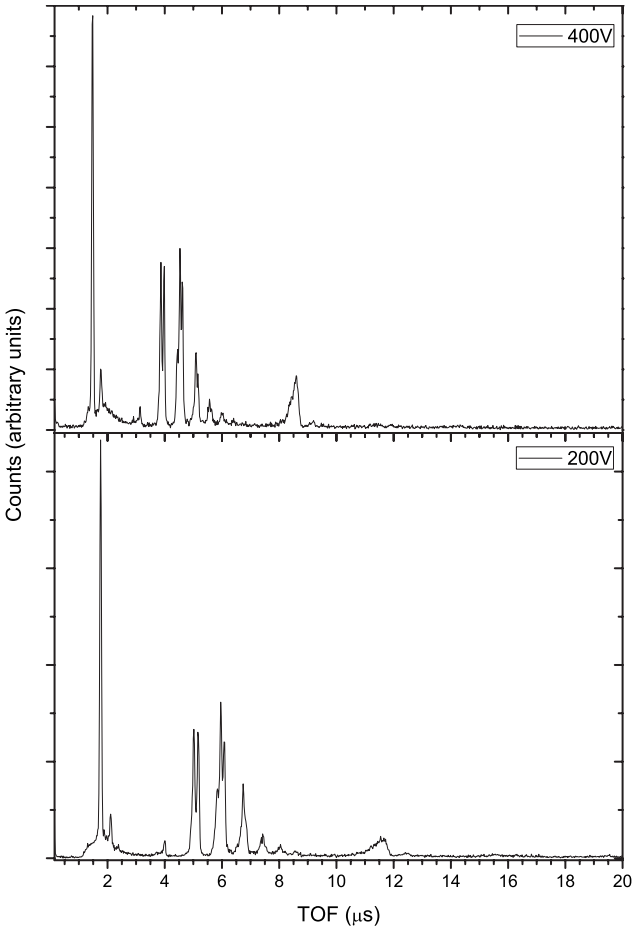

FIG. 1. TOF spectra of positive ion fragments sputtered from DDT by bombardment with Ar^{10+} ions for two different acceleration voltages +200 and +400 V.

The identification of species was made using the formula $TOF \sim (mass/V_s)^{1/2}$ [21] for each spectrum. The first observed peak in the spectra correspond to protons. By comparing the values from spectra at different sample voltages we estimated the mass resolution ($m/\Delta m$) in our configuration of around 50. For heavier molecular fragments there is some ambiguity about how many hydrogen atoms they contain.

III. RESULTS AND DISCUSSION

A. Mass spectra

Secondary ion mass spectra are displayed in Figs. 2 and 3 for irradiation with Ar^{5+} and Ar^{9+} ions, respectively, with a sample voltage of +400 V and an impact angle of 30° with respect to the normal. The spectra include both monoatomic ions and polyatomic fragment ions sputtered from the monolayer, with the corresponding molecular composition labeled for each peak.

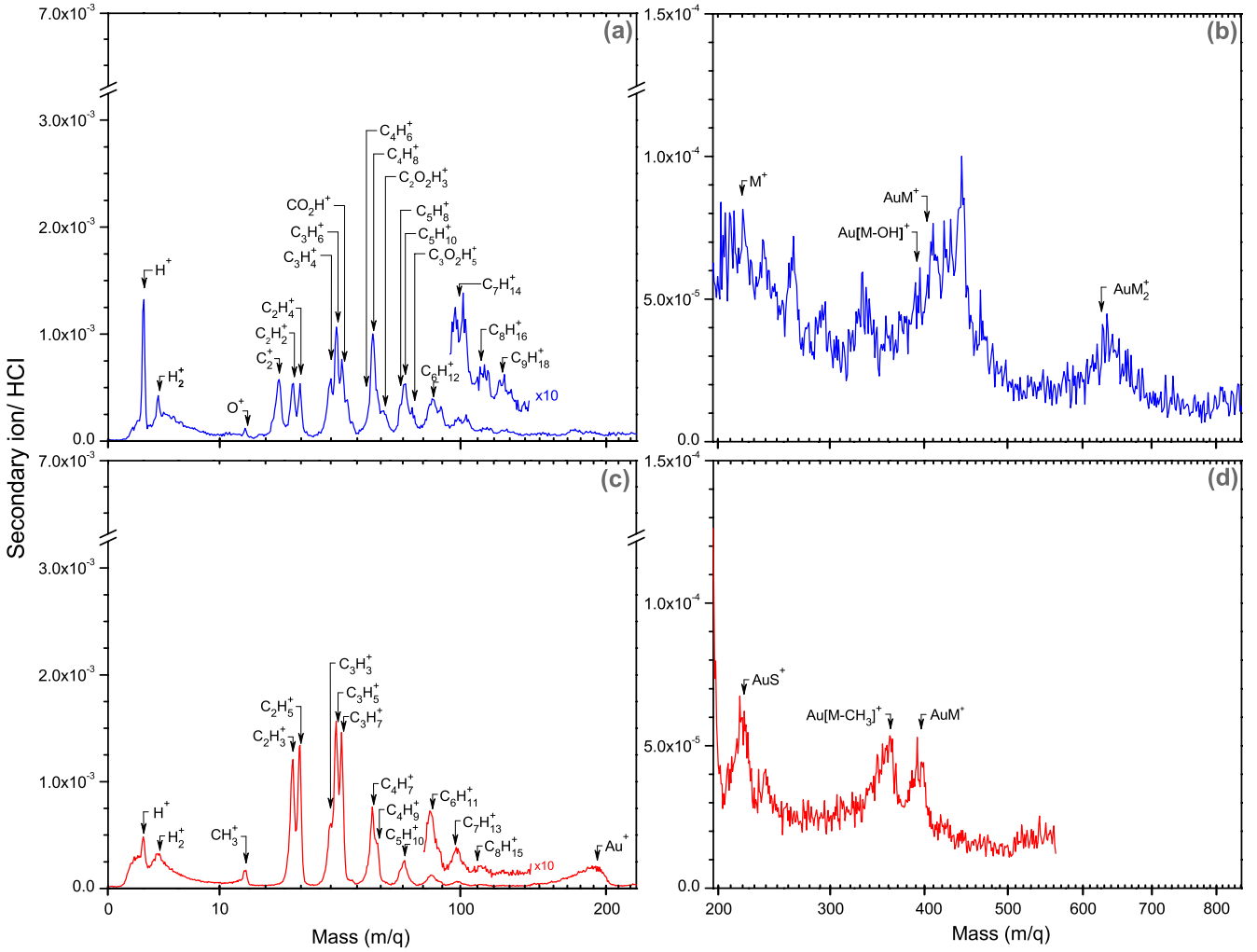

FIG. 2. (Color online) Mass spectra of secondary ions sputtered from SAM surfaces (a),(b) MUDA and (c),(d) DDT irradiated with Ar^{5+} ions at a kinetic energy of 9 keV, a sample voltage of +400 V and an incident angle of 30°. The panels on the left are composed predominantly of ionic and molecular fragments whereas the panels on the right show peaks from large mass fragments including full thiol molecules and molecule-gold clusters. The peak identification are in agreement with previous reports for single charge bombardment [9,11].

The mass spectra of positive ion fragments from MUDA are shown in Figs. 2(a), 2(b), 3(a), and 3(b). It can be seen that H^+ is the most intense for both charge state, and H_2^+ is the second most intense for Ar^{9+}. Molecular ions such as C_2^+, $C_nH_{2n}^+$, $C_{n+1}H_{2n}^+$, and fragments of the alkane chain plus functional end group $C_{n+1}O_2H_{2n+1}^+$ are also observed. In Figs. 2(b) and 3(b), the spectra of the heavier mass fragments are shown. Complete thiol molecules and molecules bound to atoms of the substrate Au$[M\text{-OH}]^+$ and AuM_n^+ (where M refers to the complete molecule) are also observed. In the case of DDT, Figs. 3(c) and 3(d), again the most intense peak in the mass spectra is associated with H^+ for Ar^{9+}, but not for Ar^{5+}, Figs. 2(c) and 2(d). Molecular ions which come from fragments of the chain $C_nH_{2n}^+$, $C_{n+1}H_{2n}^+$ and chain plus functional end group $C_{n+1}H_{2n+3}^+$ are also seen in panels (c). In the heavier mass range complete thiol molecules and molecules bound to atoms of the substrate Au$[M\text{-CH}_3]^+$ and AuM_n^+ are also observed in Figs. 2(d) and 3(d). These spectra are qualitatively in agreement with experimental and simulation results of Ar^+ bombardment of thiol-SAMs of different chain lengths [9,11].

The spectra from both SAMs show a similar peak distribution due to the chain, for both charge state. Another characteristic of the spectra is that the intensity of the molecular peaks (e.g., $C_nH_{2n}^+$) decreases monotonically with increasing molecular size from $n=3$, see panels (a) and (c), for both charge state. This behavior was also reported in the cluster emission from fullerene C_{84}-film/SiO_2/Si(100) due to bombardment with Xe^{44+} [22]. The AuM_n^+ peak intensity is more than an order of magnitude smaller than the proton intensity. The emission of complete molecule from SAM surfaces due to irradiation with singly charged ions has been reported [9]. Finally, we did not observe a sizeable Au^+ peak from the MUDA surface, as opposed to the DDT one, which might be related to reneutralization with the COOH end group. In this context it should be noted that existing density functional theory calculations [4] show that the −COOH end group contributes states at about 2.5 eV below the Fermi level as opposed to the $-CH_3$ case which contributes states at higher binding energies of more than 3.5 eV. This could make neutralization more efficient for the MUDA case.

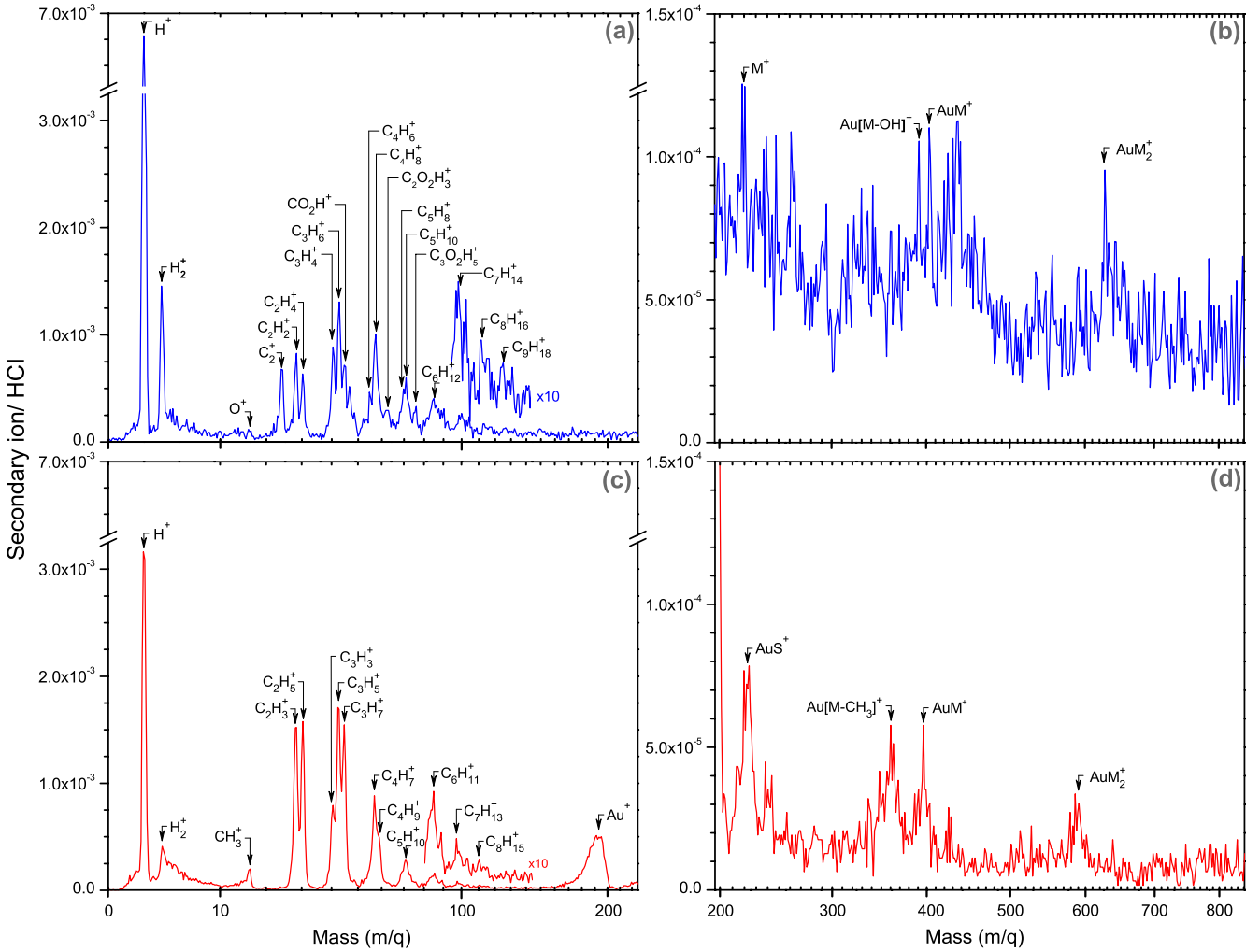

FIG. 3. (Color online) Mass spectra of secondary ions sputtered from SAM surfaces (a),(b) MUDA and (c),(d) DDT irradiated with Ar^{9+} ions at a kinetic energy of 14.4 keV, a sample voltage of +400 V and an incident angle of 30°.

It is found that, except for the proton and H_2^+ peaks, the molecular fragments yields do not show any significant charge state dependence. This is clear by compare the spectra between Figs. 2 and 3 for Ar^{5+} and Ar^{9+}, respectively. Della-Negra also reported absence of charge state effects for phenylalanin/Al [23] irradiated with highly charged argon ions.

B. Proton sputtering

The proton production as a function of the charge state is displayed in Figs. 4(a) and 4(b) for MUDA and DDT respectively. The kinetic energy of the incident ions was in the range from 2.5 to 16 keV for $4 \leqslant q \leqslant 10$ charge state. At least squared fit to the data shows that the proton yield $[Y(H^+)]$, increases with increasing charge state q with the form $Y(H^+) \propto q^\gamma$, where γ is about 5 for both SAMs. The results for each series of experiments at different kinetic energies are joined by dotted lines. For both samples the proton yields also vary with kinetic energy. For MUDA slightly different values of γ are obtained for each kinetic energy whereas for DDT essentially the same value of γ is obtained irrespective of the kinetic energy as is shown by the parallel dotted lines in the log-log plot. We shall return to this point in the following.

In an earlier paper, the q dependence of the proton sputtering yield from C_{60} surfaces with some hydrogen contamination [25] has been found to follow a power law dependence and this was explained [26] by the classical over barrier (COB) model [27]. A similar observation was made and discussed in the same manner for proton emission from hydrogenated silicon [28]. In this model a HCI approaching an atom or molecule induces multielectron transfer. In the case of our SAM it would induce electron transfer from the alkanethiol molecule functional end group. Removal of two electrons from the most external part of the SAM, would create a doubly charged chemical bond $(O\text{-}H)^{2+}$ and $(C\text{-}H)^{2+}$. Because the molecule is a poor conductor, the reneutralization probability in the molecular layer should be lower than on a metal, and a proton may be released in the bond direction by Coulomb repulsion. In general, in the above model [26] the proton yield is then dependent on the probabilities of removal of the first and second electron and on reneutralization as the ion moves away from the surface.

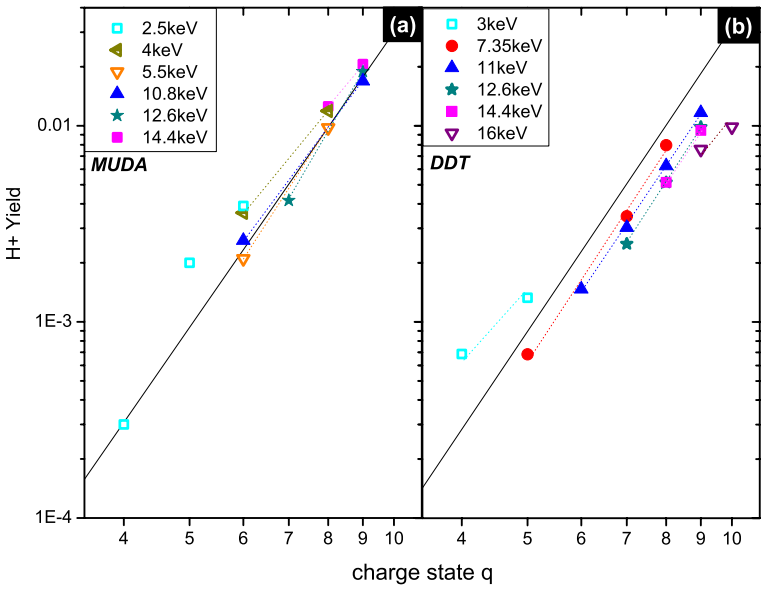

FIG. 4. (Color online) Proton yields from (a) MUDA and (b) DDT under bombardment with Ar^{q+} ions at an incident angle of 30°. For each value the error is ranged from 10–15 %. The solid line is a fit to all the data with a power law q^5. The dotted lines join data with the same kinetic energy.

The proton yields (Figs. 2–4) from MUDA are higher than those from DDT throughout the charge state and kinetic energy range studied, while *a priori* there are more hydrogen atoms in the DDT functional end group (see Fig. 5). However, the structure of the SAMs as depicted in Fig. 5 shows that the outermost layer H density is similar. The similarity between the q dependences suggests that the same mechanism governs proton emission. In this context it is interesting to compare this case with the recently investigated case of both hydrogen terminated and water terminated silicon surfaces [28–30]. The proton yields from water terminated silicon were 10 times higher than those from hydrogen terminated samples [28,30]. In Ref. [30] the larger proton yield was attributed to the relative position of the hydrogen above the hydroxylated surface, leading to a larger fraction of emitted protons surviving neutralization. The observed differences between MUDA and DDT could be related to differences in the first and second electron transfer probabilities from the two different functional groups due to differences in the electronic density of states in addition to the relative position of the hydrogen above the surface (see Fig. 5).

A series of measurements were also performed as a function of incident angle. Figure 6 shows the proton yields from MUDA and DDT surfaces from irradiation with Ar^{6+} and Ar^{8+} ions at kinetic energies of 9 and 10 keV, respectively, as a function of incident angle θ. The proton yield from DDT was larger for larger incidence angles with respect to the surface normal (smaller angle). Such a dependence was observed in HCI induced proton emission on water covered Si surface and attributed to kinetic emission [30]. On the other hand, the proton yield from MUDA showed no θ dependence. This difference could be related to the functional group orientation on the surface, with the DDT surface being locally corrugated with a proton more prominently above the surface for the DDT molecule. At the smaller HCI incidence angles with respect to the surface, this change in position relative to the MUDA case, could cause a larger probability of proton emission because the more external position of the top DDT H atom above the surface can lead to enhanced outward emission of H^+ and also to reduced neutralization probability, since ions would start further away from the surface. A discussion and simulation of some similar effects can

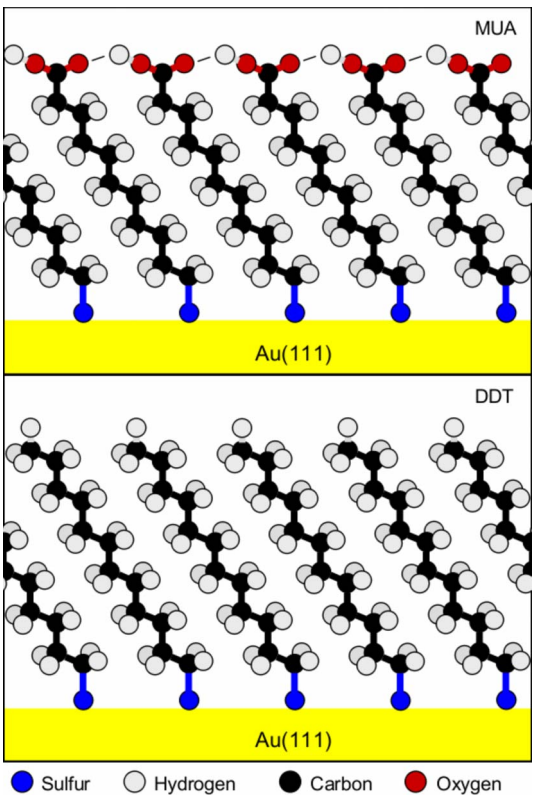

FIG. 5. (Color online) Schematic diagram of the molecular structure of the monolayer for (a) MUDA and (b) DDT [24]. In both cases one hydrogen atom is in the outermost layer. For MUDA the hydrogen atom is shown tilted to the next molecule's oxygen atom forming a weak lateral hydrogen bonding. For DDT the second line is populated by carbon and hydrogen atoms, where the C-H bond direction points into the film, but in the third line (first backbone CH_2) the C-H bond points into the vacuum. The first backbone is more exposed for DDT compared to MUDA.

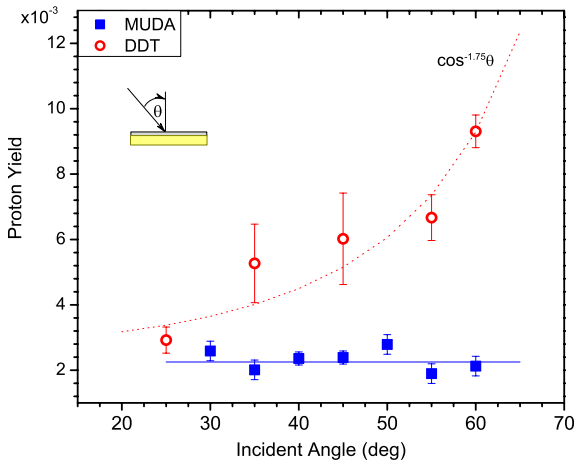

FIG. 6. (Color online) Incident angle dependence of proton yields from MUDA (full square) and DDT (empty circles) surfaces under Ar^{q+} ion irradiation, with $q=6$ and 8, respectively.

be found in our recent work on oxygen atom and ion emission on oxygen covered reconstructed silver surfaces [31].

Finally the dependence of the proton yield on the kinetic energy of the incident HCI is shown in Fig. 7 for the DDT sample. The yield decreases with increasing kinetic energy for each different HCI charge state. The neutralization of HCI over the surface is dependent on the "time above the surface." If the ions have a high velocity the time over the surface is not sufficient for complete neutralization, with further charge exchange occurring during the transit through the SAM. This can account for the observed decrease with increasing energy.

IV. CONCLUSION

We have presented results of a study of low-energy HCI interaction with MUDA and DDT SAMs. From the TOF spectra the masses of the monoatomic and polyatomic ions sputtered from the surface due to the HCI-SAM interaction were identified. The spectra were proton peak dominated. Proton yields from MUDA are generally higher than those from DDT, and proton yields increases with increasing charge state for both samples with a power law given by q^{γ}, with γ about 5 for both SAMs.

The strong charge state dependence for the proton yield is strong evidence that the protons are ejected from functional end groups as a result of multielectron transfer processes as in the COB model. Differences in the nature of the functional

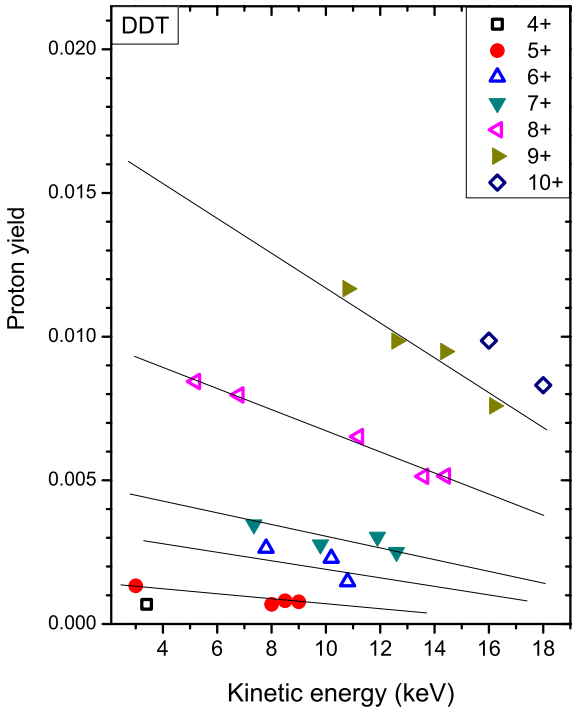

FIG. 7. (Color online) Proton yields as a function of kinetic energy for various HCI charge states for DDT.

group could lead to different contribution to proton emission due to differences in one and two electron transfer probabilities. Our results also indicate effects related to the functional group orientation on the surface. We furthermore find evidence of kinetic emission of protons, which is not the same in case of the DDT and MUDA. In all cases proton emission would be affected by neutralization processes. In case of kinetic emission from inside the SAM layer different reneutralization on the different end groups, which result in differences in the density of states, can differently affect the relative yield. This effect is invoked also to explain Au^+ emission suppression in case of the MUDA SAM.

ACKNOWLEDGMENTS

The authors thank H. Sato for his help in gold sample preparation. The authors are grateful to Professor R. Salvarezza for comments on the self-assembly of the alkanethiols. B.E.O. acknowledges support from the Japan Society for Promotion of Science. V.A.E. thanks Grant of Special Projects for Basic Science of Riken "Development and Applications of Exotic Quantum Beams" which made his stay at RIKEN possible.

[1] J. C. Love, L. A. Estroff, J. K. Kriebel, R. G. Nuzzo, and G. M. Whitesides, Chem. Rev. (Washington, D.C.) **105**, 1103 (2005); F. Schreiber, J. Phys.: Condens. Matter **16**, R881 (2004), and therein references.

[2] F. P. Zamborini, M. C. Leopold, J. F. Hicks, P. J. Kulesza, M. A. Malik, and R. W. Murray, J. Am. Chem. Soc. **124**, 8958 (2002); Y. Wang, D. Maspoch, S. Zou, G. C. Schatz, R. E. Smaley, and C. Mirkin, Proc. Natl. Acad. Sci. U.S.A. **103**, 2026 (2006).

[3] W. Wang, T. Lee, and M. A. Reed, Phys. Rev. B **68**, 035416 (2003); V. B. Engelkes, J. M. Beebe, and C. D. Frisbie, J. Am. Chem. Soc. **126**, 14287 (2004).

[4] Q. Sun, A. Selloni, and G. Scoles, J. Phys. Chem. B **110**, 3493 (2006).

[5] A. Ullman, Chem. Rev. (Washington, D.C.) **96**, 1533 (1996); F. Schreiber, Prog. Surf. Sci. **65**, 151 (2000); C. Vericat, M. E. Vela, G. A. Benitez, J. A. Martin Gago, X. Torrelles, and R. C. Salvarezza, J. Phys.: Condens. Matter **18**, R867 (2006), and therein references.

[6] G. E. Poirier, Chem. Rev. (Washington, D.C.) **97**, 1117 (1997).

[7] C. A. McDermott, M. T. McDermott, J.-B. Green, and M. D. Porter, J. Phys. Chem. **99**, 13257 (1995); D. W. Wang, F. Tian, and J. G. Lu, J. Vac. Sci. Technol. B **20**, 60 (2002); E. Ito, K. Konno, J. Noh, K. Kanai, Y. Ouchi, K. Seki, and M. Hara, Appl. Surf. Sci. **244**, 584 (2005); K. Konno, E. Ito, J. Noh, and M. Hara, Jpn. J. Appl. Phys., Part 1 **45**, 405 (2006).

[8] M. D. Porter, T. B. Bright, D. L. Allara, and C. E. D. Chidsey, J. Am. Chem. Soc. **109**, 3559 (1987).

[9] B. Hagenhoff, A. Benninghoven, J. Spinke, M. Liley, and W. Knoll, Langmuir **9**, 1622 (1993); L. Houssiau and P. Bertrand, Appl. Surf. Sci. **175**, 399 (2001); D. J. Graham and B. D. Ratner, Langmuir **18**, 5861 (2002).

[10] L. Houssiau, M. Graupe, R. Colorado, Jr., H. I. Kim, T. R. Lee, S. S. Perry, and J. W. Rabalais, J. Chem. Phys. **109**, 9134 (1998); S. S. Kim, Y. Kim, H. I. Kim, S. H. Lee, T. R. Lee, S. S. Perry, and J. W. Rabalais, *ibid.* **109**, 9574 (1998).

[11] K. S. S. Liu, C. W. Yong, B. J. Garrison, and J. C. Vickerman, J. Phys. Chem. B **103**, 3195 (1999); B. Arezki, A. Delcorte, B. J. Garrison, and P. Bertrand, *ibid.* **110**, 6832 (2006).

[12] G. Kraft, Prog. Part. Nucl. Phys. **45**, S473 (2000); S. Lacombe, C. Lesech, and V. A. Esaulov, Phys. Med. Biol. **49**, N65 (2004); C. A. Hunniford, D. J. Timson, R. J. H. Davies, and R. W. McCullough, J. Phys.: Conf. Ser. **101**, 012012 (2008).

[13] A. Arnau, F. Aumayr, P. M. Echenique, M. Grether, W. Heiland, J. Limburg, R. Morgenstern, P. Roncin, S. Schippers, R. Schuch, N. Stolterfoht, P. Varga, T. J. M. Zouros, and H. P. Winter, Surf. Sci. Rep. **27**, 113 (1997); *The Physics of Multiply and Highly Charged Ions*, edited by F. Currel (Klumer Academic, Dordrecht, 2003).

[14] J. D. Gillaspy, J. M. Pomeroy, A. C. Perrella, and H. Grube, J. Phys.: Conf. Ser. **58**, 451 (2007); F. Aumayr, A. S. El-Said, and W. Meissl, Nucl. Instrum. Methods Phys. Res. B **266**, 2729 (2008).

[15] F. Aumayr and H. Winter, Philos. Trans. R. Soc. London, Ser. A **362**, 77 (2004).

[16] T. Schenkel, M. Schneider, M. Hattass, M. W. Newman, A. V. Barnes, A. V. Hamza, D. H. Schneider, R. L. Cicero, and C. E. D. Chidsey, J. Vac. Sci. Technol. B **16**, 3298 (1998).

[17] L. P. Ratliff, R. Minniti, A. Bard, E. W. Bell, J. D. Gillaspy, D. Parks, A. J. Black, and G. M. Whitesides, Appl. Phys. Lett. **75**, 590 (1999).

[18] A. Endo, N. Nakamura, Y. Kanai, Y. Nakai, K. Komaki, and Y. Yamazaki, Nucl. Instrum. Methods Phys. Res. B **205**, 187 (2003); N. Nakamura, M. Terada, A. Endo, Y. Nakai, Y. Kanai, K. Komaki, and Y. Yamazaki, J. Phys.: Conf. Ser. **2**, 1 (2004); N. Nakamura, Y. Nakai, Y. Kanai, K. Komaki, A. Endo, and Y. Yamazaki, Rev. Sci. Instrum. **75**, 3034 (2004).

[19] N. Okabayashi, K. Komaki, and Y. Yamazaki, Nucl. Instrum. Methods Phys. Res. B **205**, 725 (2003); **235**, 438 (2005).

[20] M. H. Dishner, M. M. Ivey, S. Gorer, J. C. Hemminger, and F. J. Feher, J. Vac. Sci. Technol. A **16**, 3295 (1998); C. Nogues and M. Wanunu, Surf. Sci. **573**, L383 (2004).

[21] N. Okabayashi, K. Komaki, and Y. Yamazaki, Nucl. Instrum. Methods Phys. Res. B **235**, 438 (2005).

[22] T. Schenkel, A. V. Barnes, A. V. Hamza, and D. H. Schneider, Eur. Phys. J. D **1**, 297 (1998); A. V. Hamza, T. Schenkel, and A. V. Barnes, *ibid.* **6**, 83 (1999).

[23] S. Della-Negra, J. Depauw, H. Joret, Y. Le Beyec, and E. A. Schweikert, Phys. Rev. Lett. **60**, 948 (1988).

[24] The molecular arrangement of the alkanethiols has been discussed for several authors, for example, R. Arnold, W. Azzam, A. Terfort, and C. Woll, Langmuir **18**, 3980 (2002), for the COOH end group and B. Li, C. Zeng, Q. Li, B. Wang, L. Yuang, H. Wang, J. Yang, J. G. Hou, and Q. Zhu, J. Phys. Chem. **107**, 972 (2003), for the CH_3 end group.

[25] N. Kakutani, T. Azuma, Y. Yamazaki, K. Komaki, and K. Kuroki, Jpn. J. Appl. Phys., Part 2 **34**, L580 (1995); Nucl. Instrum. Methods Phys. Res. B **96**, 541 (1995).

[26] J. Burgdorfer and Y. Yamazaki, Phys. Rev. A **54**, 4140 (1996).

[27] A. Niehaus, J. Phys. B **19**, 2925 (1986); J. Burgdorfer, P. Lerner, and F. W. Meyer, Phys. Rev. A **44**, 5674 (1991).

[28] K. Kuroki, N. Okabayashi, H. Torii, K. Komaki, and Y. Yamazaki, Appl. Phys. Lett. **81**, 3561 (2002); K. Kuroki, H. Torii, K. Komaki, and Y. Yamazaki, Nucl. Instrum. Methods Phys. Res. B **193**, 804 (2002).

[29] K. Kuroki, K. Komaki, and Y. Yamazaki, Nucl. Instrum. Methods Phys. Res. B **203**, 183 (2003).

[30] N. Okabayashi, K. Komaki, and Y. Yamazaki, Nucl. Instrum. Methods Phys. Res. B **232**, 244 (2005).

[31] L. Guillemot, Y. Bandurin, K. Bobrov, and V. A. Esaulov, J. Phys.: Condens. Matter **20**, 355008 (2008).